

A CMOS Multi-band Low Noise Amplifier Using High-Q Active Inductors

Ming-Jeui Wu, Yuan-Hao Lee, Yi-Yuan Huang, Yu-Min Mu and Jenn-Tzer Yang

Abstract—In this paper, a CMOS Multi-band LNA using High-Q active inductors load with a binary code band selector suitable for multi-standards wireless applications is proposed. Using an improved high-Q active inductor including two bits binary controlled code, the multi-band low noise amplifier operating at four different frequency bands is realized. The proposed amplifier is designed in TSMC 0.18-um CMOS technology. Based on the simulation results, the amplifier can operate at 900MHz, 1.8GHz, 1.9GHz, and 2.4GHz with forward gain (S_{21}) of 40.7dB, 35.9dB, 37.2dB, and 30.7dB, and the noise figure (NF) of 0.018dB, 0.006dB, 0.001dB, and 0.01dB, respectively. Furthermore, the power dissipation of this amplifier can retain constant at all operating frequency bands and consume around 10.53 mW from 1.8-V power supply.

Keywords—CMOS, High-Q Active Inductor, Low Noise Amplifier, Multiple Band, and Multi-Standards.

I. INTRODUCTION

IN recently years, the evolution of wireless communications has motivated a strong interest toward the development of multi-standards and multi-services with operating frequencies of 0.9GHz/1.8GHz/1.9GHz bands for GSM and 2.4GHz band for Bluetooth. Therefore, it is desirable to combine more standard bands in one mobile unit [1]. Typical design strategies have used different amplifiers for different frequency bands [2]-[3]. Using option control to do frequency selected receiver [4], [5], [8]. Use differential LNA to GSM and Bluetooth Receiver. The differential type can increase gain and reduce NF value [6]-[7]. Applying high-Q active inductor can make LNA circuit get better character. In this paper, a non-inductor RF multi-band low noise amplifier using TSMC 0.18-um CMOS technology applying high-Q active inductor with binary code band selector for multi-standards or multi-services is presented.

The amplifier exhibits constant power consumption at all operating frequency bands and can operate at 0.9GHz, 1.8GHz, 1.9GHz, and 2.4GHz four frequency bands selecting capability. The organization of this paper is described as follows. Constant power consumption with a band selectable high-Q active

inductor is described in section 2. In section 3, the circuit of the band selector using two bits binary code is proposed. The proposed multi-band low noise amplifier using the high-Q active inductor with steady power consumption and multi-band frequency selecting is introduced in section 4. Simulation results of the proposed multi-band low noise amplifier are indicated in section 5. Finally, the conclusion is summarized in section 6.

II. ACTIVE INDUCTOR WITH BAND SELECTOR

The simple grounded active inductor circuit and its equivalent circuit are shown in Fig.1. Each MOS transistor is modelled by the equivalent device components including g_m , g_{ds} , C_{gs} , and C_{gd} . Assumed that $g_m \gg g_{ds}$ and $C_{gs} \gg C_{gd}$ are established, and then the equivalent input impedance (Z_{in}) of this inductor can be derived as Eq. (1). According to the Eq. (1), the conductance (G) values and the inductance (L) of the inductor are expressed from Eq. (2) and Eq. (3). The Q value and the resonant frequency ω_0 are shown in Eq. (4) and Eq. (5), respectively. Were g_{mi} , g_{dsi} , and C_{gsi} are the transconductance, the output conductance, and the gate-source capacitance of correspondence transistors, respectively. By Eq. (2), the increasing parallel conductance loss of (G) will reduce the Q value of the inductor. Therefore, in order to improve the performance such as the Q value, a high-Q active inductor using a feedback resistor is proposed.

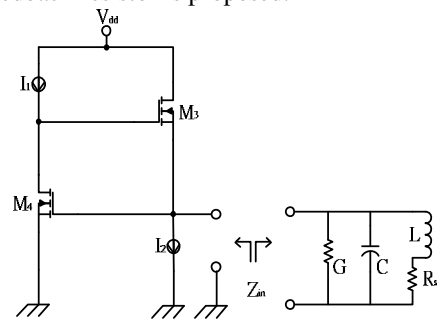


Fig. 1 Simple active inductor and equivalent circuit

$$Z_{in} \approx \frac{(g_{ds3} + g_{m4}) + S(C_{gs3} + C_{gd4} + C_{gd3})}{(SC_{gd3} + g_{ds3} + g_{m4})(S(C_{gs3} + C_{gd4}) + g_{m3})} \quad (1)$$

$$G \approx g_{ds3} + g_{m4} \approx g_{m4} \quad (2)$$

$$L \approx \frac{C_{gs3}}{g_{m4} g_{m3}} \quad (3)$$

Ming-Jeui Wu is with the Ming Hsin University of Science and Technology, Department of Electronics Engineering (e-mail: mrwu@must.edu.tw)
Yuan-Hao Lee is with the Ming Hsin University of Science and Technology, Department of Electronics Engineering (e-mail: c95030019@std.must.edu.tw)
Yi-Yuan Huang is with the Ming Hsin University of Science and Technology, Department of Electronics Engineering (e-mail: c95030003@std.must.edu.tw)
Yu-Min Mu is with the Ming Hsin University of Science and Technology, Department of Electronics Engineering (e-mail: c95030020@std.must.edu.tw)
Jenn-Tzer Yang is with the Ming Hsin University of Science and Technology, Department of Electronics Engineering (e-mail: yjn@must.edu.tw)

$$Q \approx \sqrt{\frac{g_{m4} g_{m3} C_{gs3}}{g_{ds4}^2 C_{gs4}}} \quad (4)$$

$$\omega_0 \approx \sqrt{\frac{g_{m4} g_{m3}}{C_{gs4} C_{gs3}}} \quad (5)$$

The improved high-Q active inductor circuit is illustrated in Fig. 2. This circuit is composed of common-source transistor M_4 , common-drain transistor M_3 , feedback resistor R_f and two biasing current sources I_1 and I_2 . Feedback resistor and transistor M_4 construct a gain network. This network produces a gain factor to reduce the parallel conductance loss (G). Hence, the equivalent internal loss of the inductor will be decreased, and then the Q value will be increased. Moreover, the inductance (L) is also increased due to the feedback resistor. At high frequency, this circuit is equivalent to a resonator as well, which is the same as Fig. 1(b). The conductance (G) values and the inductance (L) of this inductor including three parameters, C_{gs1} , g_{ds1} , and g_{mi} are derived as Eq. (6) and Eq. (7). The Q value and the resonant frequency ω_0 are shown in Eq. (8) and Eq. (9), respectively.

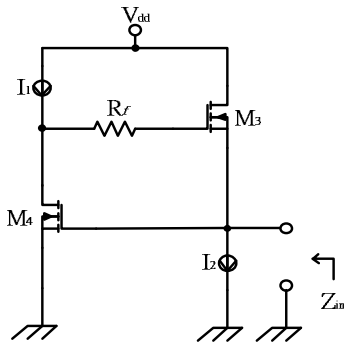


Fig. 2 High-Q active inductor

$$G \approx \frac{g_{m4}}{1 + R_f g_{ds4}} \quad (6)$$

$$L \approx \frac{C_{gs3} (1 + R_f g_{ds4})}{g_{m4} g_{m3}} \quad (7)$$

$$Q \approx \sqrt{\frac{g_{m4} g_{m3} C_{gs3}}{g_{ds4}^2 C_{gs4}} \times (1 + R_f g_{ds4})} \quad (8)$$

$$\omega_0 \approx \sqrt{\frac{g_{m4} g_{m3}}{C_{gs4} C_{gs3} (1 + R_f g_{ds4})}} \quad (9)$$

By Eq. (6) and Eq. (7), the effect of the factor, $(1 + R_f g_{ds4})$, is designed to be a value greater than unity. This factor will result in the equivalent conductance loss (G) to be minimized and the equivalent inductance (L) to be increased as well. From Eq. (8) and (9), the Q-value is promoted with the feedback resistance

by the $\sqrt{1 + R_f g_{ds4}}$ factor and the resonant frequency ω_0 is inverse proportion of the $\sqrt{1 + R_f g_{ds4}}$ factor.

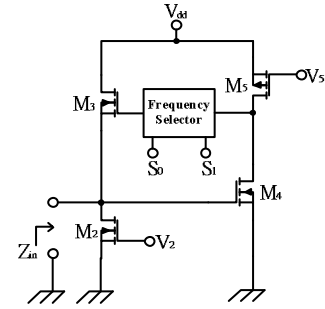


Fig. 3 High-Q active inductor circuit with band selector

In order to change the characteristics of the active inductor, the active inductor can use a simple network to control the feedback resistance. In Fig.3 this simple network, the different feedback resistances can be selected by using binary code to form a band selector. The band selector can choose all kinds of resistance using different binary code, and then the inductance, the Q-value, and the resonating frequency ω_0 of the inductor will be changed.

III. BANDS SELECTOR CIRCUIT

In Fig. 4 shows the band selecting configuration to replace the feedback resistor. It is formed by using six transmission gates and two inverters to select the resistance. As input binary code ($S_1 S_0$) of the multiplex apply with individual 00, 01, 10, and 11, and then the feedback resistance of R_{2400} , R_{1900} , R_{1800} , and R_{900} will be selected respectively.

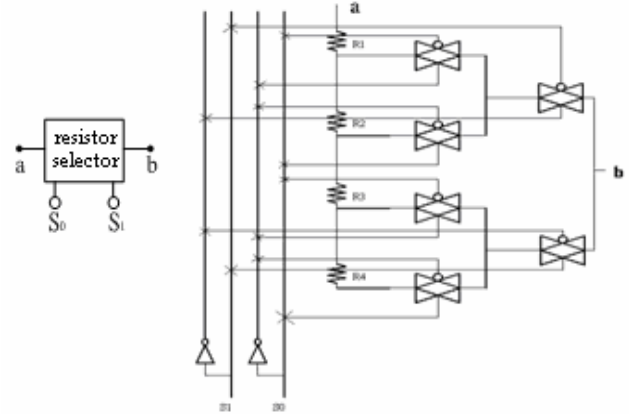


Fig. 4 The Bands selector circuit

Moreover, the proposed active inductor, due to the DC bias current does not pass through the band selector. The voltage drop of the band selector is zero. Hence, the DC voltage drop of the band selector will not be affected the characters of the inductor during the feedback resistor is changed. Therefore, the power consumption of the active inductor can be retained constant.

IV. PROPOSED MULTI-BAND LNA DESIGNS

An active inductor can apply in a constant low power multi-band amplifier design to obtain. It is included four

advantages, there are bands change easily, obtain multiple bands, high gain and constant power consumption. Typically, the inductance load is applied with a passive spiral inductor. However, inherently low Q-factors and occupied large chip area, the gain and the cost-performance of the amplifier designs will be significantly decreased. Hence, an active inductor can employ in the load of the amplifier to improve above these disadvantages.

$$Z_{in} \approx \frac{1}{(g_{ds1} + g_{m2} + j\omega C_{gs2} + j\omega C_{gd1})} \approx \frac{1}{g_{m2}} \quad (10)$$

In the Fig5, the main framework of the circuit of the differential amplifier consists of one input port and two outputs port. Large gain and low noise figure (NF) can be obtained on the two-stage output. On the left-handed side of the framework is a common gate, a common source, an active inductor and a buffer. On the right-handed side have a common source, an active inductor and a buffer. M_1 is the transistor of the common gate of the input stage which can be easily matched. In the common-gate configuration, transistors M_1 and M_2 are employed as the input stage for input impedance matching. The input impedance (Z_{in}) of this amplifier can be approximated as Eq. (10). Where g_{mi} , g_{dsi} , and C_{gsi} are the transconductance, the output conductance, the gate-source capacitance of correspondence transistors, respectively. Hence, the input matching of the amplifier can be easily achieved by setting $1/g_{m2}$. The Q value of the active inductor is high, enhancing the performance of the circuit. M_4 and M_{13} are common-source type of transistors through which an inverse output waveform is obtained. $M_6 \sim M_9$ are the transistors of the buffer for output match.

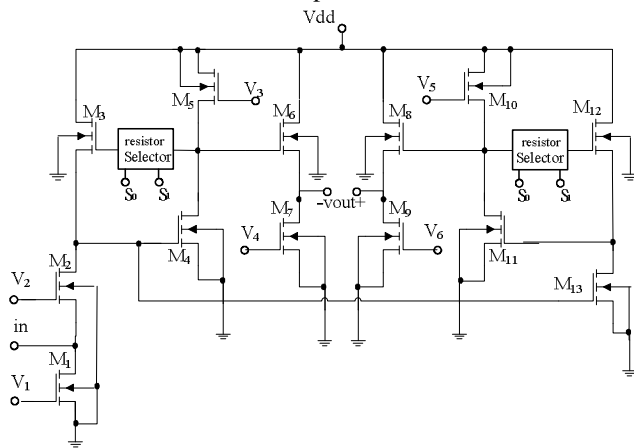


Fig. 5 Proposed RF multi-band low noise amplifier

The operation of the circuit on the right-handed side is that a signal, fed into the M_1 common gate and passing through the load of the inductor and the M_4 common source, turns into an inverse signal and then arrives at M_7 through the buffer. The output is the inverse of the input and is therefore marked as V_{out-} . The operation on the left-handed side is that the signal coming out of the M_1 common source becomes the input of the M_{13} common source and its phase is reversed for 180° . The reversed signal, going through the M_{11} common source, is reversed again for the phase change of 180° and then is

outputted into M_9 after passing the buffer. The final output is in phase with the original input and is therefore marked as V_{out+} .

A large gain of differential output is obtained from V_{out+} and V_{out-} because of their phase difference of 180° . The common gate and common source do not change the phase of NF. If the NF value of two output ports is more close, the NF difference outputs will be very small.

V. SIMULATION RESULTS

The proposed high-Q active inductor and the RF multi-band low noise amplifier were designed in standard TSMC 0.18-um CMOS technology. The simulation tool of ADS (advanced design system) was applied in these designs. It is desirable that the frequency bands of the amplifier design can be selected by selecting the feedback resistance in band selector to obtain four different frequency bands. The bands are includes 0.9GHz, 1.8GHz, 1.9GHz, and 2.4GHz. At these frequency bands, the forward gain, the input (S_{11}) and the output (S_{22}) (S_{33}) reflection coefficients are displayed in Fig6, 7, 8 and 9, respectively.

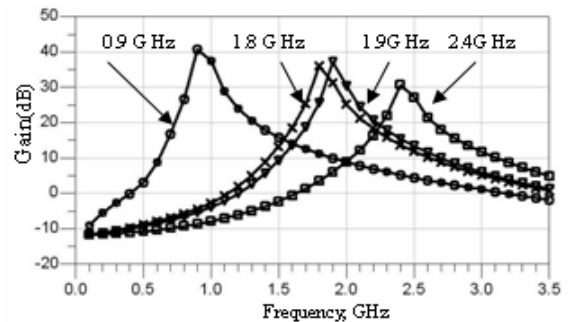


Fig. 6 Gain of proposed amplifier

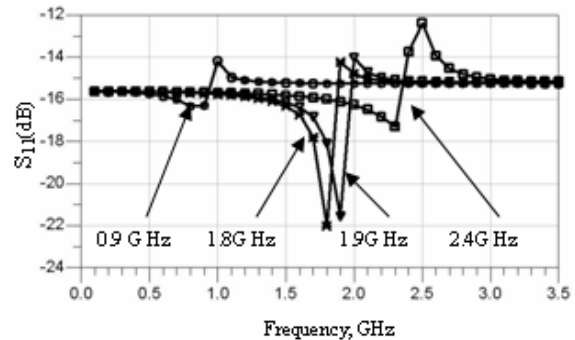


Fig. 7 Input matching (S_{11}) of proposed amplifier

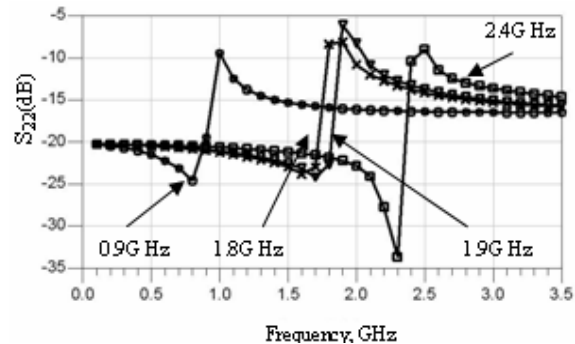


Fig. 8 Output matching (S_{22}) of proposed amplifier

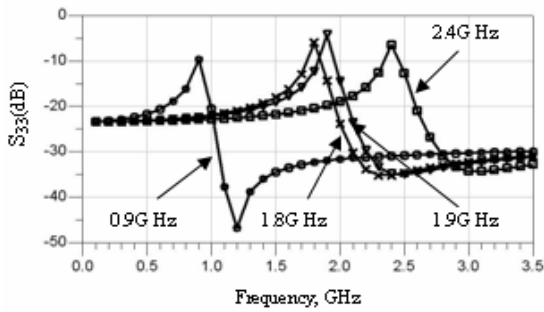


Fig. 9 Output matching (S_{33}) of proposed amplifier

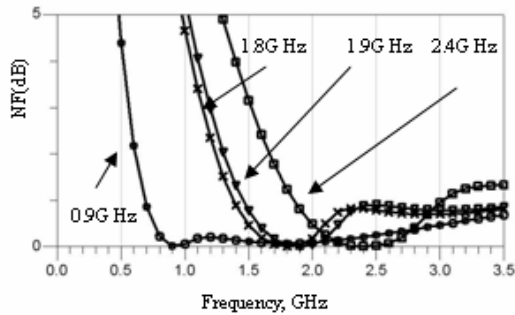


Fig. 10 Noise figure (NF) of proposed amplifier

Frequency	2.4 GHz	1.9 GHz	1.8 GHz	0.9 GHz
Gain (dB)	30.7	37.2	35.9	40.7
nf(2) (dB)	17.49	17.278	17.264	17.072
nf(3) (dB)	17.5	17.277	17.258	17.054
NF (dB)	0.01	0.001	0.006	0.018
S11 (dB)	-13.7	-21.5	-22	-16.3
S22 (dB)	-10.4	6.12	-8.3	-19.5
S33 (dB)	-6	-4.2	-5.9	-9.6
I	5.85 (mA)			
Power	10.53 (mW)			

* nf(2) is NF of the vout+ ; nf(3) is NF of the vout-

Table 1. This work performances

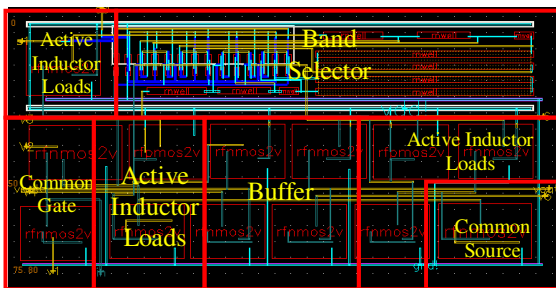


Fig. 11 Layout of proposed amplifier

In the Fig 6, the selected frequency bands of 0.9GHz, 1.8GHz, 1.9GHz, and 2.4GHz, with the forward gain can achieve 40.7dB, 35.9dB, 37.2dB, and 30.7dB, respectively. In Fig 7, 8 and 9, the input and the output reflection coefficients

are smaller than -13dB, -6.1 dB and -4.2dB, respectively. In Fig. 10 the noise figure (NF) at four frequency bands is less than 0.018dB. Fig. 11 is the layout of the proposed amplifier.

Finally, to validate our analysis an LNA is integrated in a 0.18um CMOS process which performances are summary in table 1. The simulated results obtained for the designed LNA, are summary in the table 2. Compared to previous published works [4-6] and taking into account that the amplifier is fully integrated, the overall performances appear very good.

	[4]	[5]	[6]	This Work
Frequencies (GHz)	2.4	1.9 & 2.4	2.4	0.9 & 1.8 & 1.9 & 2.4
Technology (COMS)	0.18- μ m	0.18- μ m	0.18- μ m	0.18- μ m
power supply	1.8V	1.8V	1.5V	1.8V
Gain (dB)	10 ~ 18	15 ~ 17	18.9	30.7 ~ 40.7
NF (dB)	1.5 ~ 4.45	2.2 ~ 2.25	2	0.001 ~ 0.018
S11 (dB)	-4.2 ~ -15	-14 ~ -16	-10.62	-13.7 ~ -22
S22 (dB)			-9.6	-6.12 ~ -19.5
I (mA)	-	4 & 8	-	5.85
Power (mW)	6.2	7.2 & 13.1	-	10.53

Table 2. LNAs performances

VI. CONCLUSION

In this study, an active inductor multi-band low noise amplifier with steady power consumption is obtained. The amplifier can operate at four different frequency bands, which uses two bits binary controlled codes for GSM and Bluetooth applications. In this amplifier, operating at the selected frequency bands, the enough forward gain, the reasonable input and output reflection coefficients, and the low noise figure can be obtained. Furthermore, the constant low power consumption of 10.53 mW under 1.8V DC power supply and the small occupied chip area 158 x 76 mm² are achieved.

REFERENCES

- [1]. T. Antes and C. Conkling, "RF chip set fits multimode cellular/PCS handsets," Microwave RF, PP. 177-186, Dec. 1996.
- [2]. S. Wu and B. Razavi, "A 900-MHz/1.8-GHz CMOS receiver for dual-band applications," IEEE J. Solid-State Circuits, vol. 33, no. 12, pp. 2178-2185, Dec. 1998.
- [3]. R. Magoon, I. Koullias, L. Steigerwald, W. Domino, N. Vakillian, E. Ngompe, M. Damgaard, K. Lewis, and A. Molnar, "A triple-band 900/1800/1900 MHz low-power image-reject front-end for GM," ISSCC Dig. of Tech. Papers, San Francisco, USA, Feb. 2001, pp.408-409.
- [4]. Kuo-Hua Cheng Christina F. Jou .A Novel Gain Control LNA for 2.4GHz Application using 0.18um CMOS
- [5]. Vidojkovic, V.; van der Tang, J.; Hanssen, E.; Leeuwenburgh, A.; van Roermund. Fully - Integrated DECT/Bluetooth Multi-band LNA in 0.18 um CMOS . Volume 1, 23-26 May 2004 Page
- [6]. Shaikh K. Alam and Joanne DeGroat .A 1.5-V 2.4 GHz Differential CMOS Low Noise Amplifier for Bluetooth and Wireless LAN Applications
- [7]. C.-P. Chang, C.-C. Yen, and H.-R. Chuang. A 0.18um 2.4 - 6 GHz CMOS Broadband Differential LNA for WLAN and UWB Receiver
- [8]. Z. Li, R. Quintal and K. K. O., "A dual-band CMOS front-end with two gain modes for wireless LNA applications," IEEE J. Solid-State Circuits, vol. 39, no. 11, pp. 2069-2073, Nov. 2004.